Structural and sub-structural features of chemically deposited Zinc-oxide thin films

A. S. Opanasyuk*[a], T. O. Berestok[a], P. M. Fochuk[b], A. E. Bolotnikov[c], and R. B. James[c]
[a] Sumy State University, Rimsky-Korsakov Str., 2, Sumy, Ukraine;
[b] Chernivtsi National University, Kotsyubynskogo Str., Chernivtsi, Ukraine;
[c] Brookhaven National Laboratory, USA

ABSTRACT

We investigated the structural and sub-structural characteristics of ZnO films obtained by chemical bath deposition from solutions of zinc sulfate, thiourea, and ammonia. The duration of deposition ranged from 20- to 120-minutes. The concentration of thiourea was varied from 0.1- to 3-mol. We detailed the structural and sub-structural characteristics of these films using high-resolution scanning electron microscopy and x-ray diffraction. This research enables us to study features of the films' structural formation, and to determine their basic characteristics, viz., phase analysis, texture quality, lattice constants, grain size, and size of the coherent scattering domain. Regimes were identified for depositing films with optimal structural characteristics for eventual use in solar-energy applications.

Keywords: Zinc oxide, chemical bath deposition, surface morphology, structure, sub-structure, X-ray diffraction

INTRODUCTION

Increasingly, zinc oxide is attracting the attention of researchers due to its unique properties and the possibility of its application as the base material in a variety micro-, optical- and acoustic-electronic devices. This material has high transparency in the visible spectrum, low toxicity, chemical- and thermal-stability, and good biocompatibility [1]. Moreover, due to the material's high exciton-binding energy (60 meV), effective laser generation is expected at room temperature [2]. Also, zinc oxide has a large band gap (E_g = 3.37 eV); consequently, it effectively absorbs ultraviolet radiation and so can be used as a sensor of UV radiation [3]. Furthermore, ZnO films are widely used as conductive- and window-layers of large-area solar cells [4].

Numerous growth techniques have been used to produce ZnO thin films including molecular-beam epitaxy [5], vapor deposition [6], magnetron sputtering [7], spray pyrolysis [8], and the sol-gel method [9]. Most of these processes are characterized by high complexity, and they necessitate use of high vacuum, energy or temperature during synthesis. Nowadays, chemical bath deposition (CBD) [10-15] is one of the most promising methods for obtaining ZnO films. Its main advantages are simplicity and efficiency, requiring only low temperature and pressure during synthesis, and, also affording the possibility of obtaining of large-areal layers on substrates of different shapes. Moreover, this method is suitable for depositing ZnO films with controllable structural properties, such as nanocrystalline layers, nanorods, and nanosheets. [10,12-14]

To generate ZnO layers, we employ different chemical reagents as precursors. Other researchers [10-13] have obtained zinc-oxide films from solutions of zinc nitrate and hexamethylenetetramine (HMTA) [10-11], hexamethylenetetramine and ammonia [12], and ethylenediamine and trietanolamine [13]. In contrast, in making the films, we employed a more accessible solution of zinc sulphate ($ZnSO_4$), thiourea ($CS(NH_2)_2$) and ammonia (NH_4OH), the latter serving as a complex agent to control sedimentation. The aim of our work was to study the structural- and sub-structural-characteristics of the condensates. These condensates were conditional upon our choice of the concentration of thiourea, the duration of the deposition, and the selection of optimum deposition conditions used to obtain films with the desired structural characteristics.

EXPERIMENTAL DETAILS

We generated ZnO films by chemical bath deposition by immersing the glass substrate in a chemical reactor with the aqueous precursors heated to 368 K. We prepared the initial solution by adding 50 ml of 0.1-M zinc sulfate dihydrate ($ZnSO_4 \cdot 2H_2O$) and 50-ml thiourea ($CS(NH_2)_2$) at concentrations of 0.1M, 0.5M, 1M, 2M, and 3M. The pH was

Thin Film Solar Technology V, edited by Louay A. Eldada, Michael J. Heben, Proc. of SPIE
Vol. 8823, 88230Q · © 2013 SPIE · CCC code: 0277-786X/13/$18 · doi: 10.1117/12.2023238

maintained at 10 by adding 10 ml of 25% ammonia solution (NH_4OH). The duration of deposition, τ, varied from 20- to 120-min. The substrates previously were cleaned with KOH, then isopropyl alcohol, and finally, distilled water.

The structure of the films was investigated via the X-ray diffractometer DRON 4-07 (Ni-filtered K_α – radiation of Cu-anode). The spectra were registered in the angle range $2\theta = 20^0$-80^0 (2θ - the Bragg angle). We focused the x-ray radiation according to the Bragg-Brentano method [16]. The phase analysis was accomplished by comparing the inter-plane distances and specific intensities of the XRD patterns of the samples, and from powder-diffraction data [17].

Harris' method was used to determine the film's texture. It especially is convenient for plane specimens where the axis of the texture is oriented normal to the surface tested [18]. The pole-density value was calculated via the equation:

$$P_i = \frac{(I_i / I_{0i})}{\frac{1}{N}\sum_{i=1}^{N}(I_i / I_{0i})},$$

where I_i, I_{0i} – are the integral intensities of i-diffraction peak of the sample and etalon; N is the number of lines in the XRD pattern.

Thereafter, on the basis of this calculation, we built the dependencies $P_i - \varphi$ (where φ - is an angle between chosen direction and the normal to different crystallographic planes corresponding to the reflexes in the XRD patterns), and P_i – $(hkl)_i$ (where $(hkl)_i$ – Miller indexes). The angle φ was calculated for the hexagonal lattices according to equations given in [18]. The axis of the texture has values corresponding to the maximum P_i. The orientation factor was computed as $f = \sqrt{\frac{1}{N}\sum_{i=1}^{N}(P_i - 1)^2}$.

The interplane distances for the wurtzite phases of the ZnO were obtained from the position of the $K_{\alpha 1}$ component of all of the most intense lines registered in the XRD-patterns. To determine the lattice parameters, a and c, of the hexagonal phase for ZnO, we used the following expressions:

$$a = \frac{\lambda}{2\sin\theta}\sqrt{\frac{4}{3}(h^2 + hk + k^2) + \left(\frac{a}{c}\right)^2 l^2}, \quad (1)$$

$$c = \frac{\lambda}{2\sin\theta}\sqrt{\frac{4}{3}\left(\frac{c}{a}\right)^2 (h^2 + hk + k^2) + l^2}, \quad (2)$$

where λ – is the X-ray wavelength.

The ratio c/a was considered equal to the value defined in the reference $c/a = 1.601$ [17]. Further, to gain precise values of the lattice constants, we followed the extrapolation method of Nelson-Riley [19, 20]. The least-squares method yielded a linear approximation of the points. For specifying the a and c constants of the hexagonal phase, we used a graphical method of successive approximations [18], repeating the calculations until the value of a, c, and c/a converged.

To determine the size of the coherent scattering domain (CSD) L in compounds, we used the Scherrer equation [16]: $L = \frac{K\lambda}{\beta\cos\theta}$, where the K - coefficient depended on the grain's shape ($K = 0.94$), and on β - the physical broadening of the X-ray line [19, 21].

RESULTS AND DISCUSSION

Figure 1 shows the electron-microscopic images of the surface of ZnO films obtained after different durations of deposition. It shows that the condensates, deposited for 20 minutes, are nanorods formed as hexagonal prisms with dimensions: $d = (0.25\text{-}1.00)$ μm in diameter and $l = (2.50\text{-}3.00)$ μm in length. They grow at different angles to the substrate. With increasing condensation time (from 60- to 120-minutes), due to the secondary nucleation there took place splice of intervals between nanorods and formation of continues film.

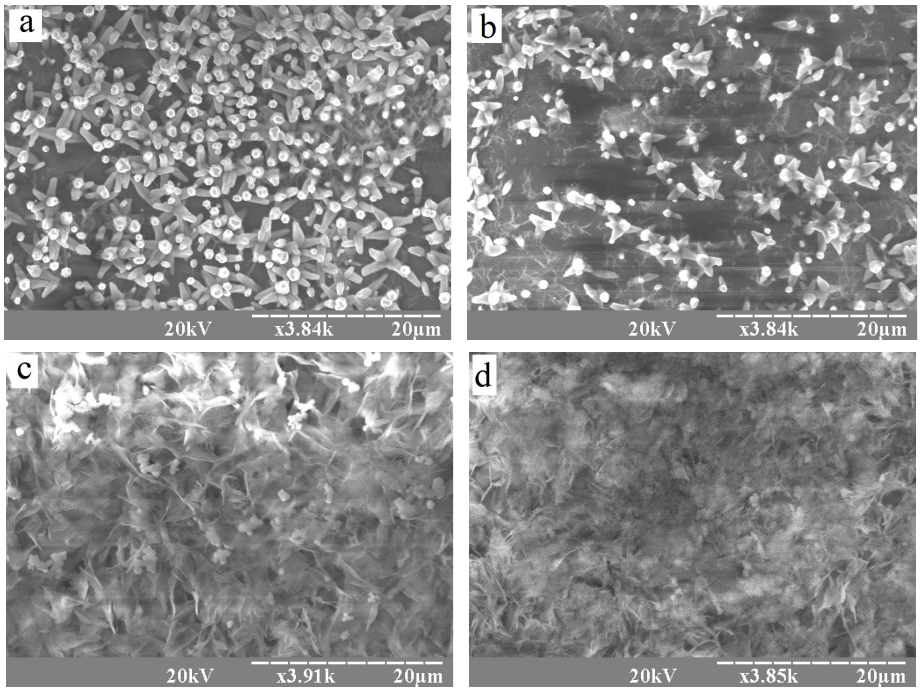

Figure 1. SEM micrographs of ZnO obtained after different durations of deposition: a,b: τ=20 min, c: 90 min, d: 120 min

Phase analysis of the XRD patterns for the condensates deposited at different concentrations of thiourea (τ = 60 min) showed that layers have a hexagonal structure. In the X-ray patterns, the intensities of reflections at angles (36.36^0–36.38^0) were the largest ones. The diffraction peaks correspond to the reflections from the (002) plane of the hexagonal phase of ZnO. This finding points to textured growth of the films.

Along with these peaks, we registered very intense lines at the angles 31.66^0, 36.16^0, and 62.72^0 that were identified as the reflections, respectively, from (100), (101), and (110) planes of the ZnO wurtzite phase [17].

In addition in some XRD patterns, we discerned peaks at angles (24.65^0–24.65^0) that have been identified by others as a reflection of the (002) plane of $Zn_4SO_4(OH)_6\ H_2O$ compound. We note that annealing the layers in vacuum caused the decomposition of this compound [12].

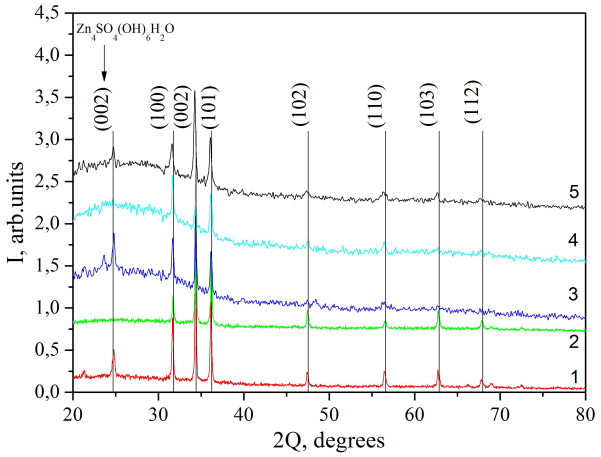

Figure 2. XRD patterns of films obtained at different concentrations of thiourea (1 - 0.1 M, 2 - 0.5 M, 3 – 1 M, 4 – 2 M, 5 – 3 M) and duration of the deposition of τ = 60 min

The growth of the films' texture was confirmed by calculations of the reverse pole figures. The results of this assessment are depicted in Figure 3(a); they reveal that the pole density has a maximum value for the crystallographic (002) plane of ZnO hexagonal phase, indicating the existence of [002] texture. This growth texture is atypical for zinc oxide, which most often, has a growth texture in the [100] direction [10, 11]. Similar textural growth [002] was observed by others [12], wherein zinc oxide films were prepared by chemical-bath deposition from solutions of zinc nitrate and ammonia. Figure 3(b) displays the dependence of the orientation factor on the concentration of thiourea. We found that increasing the concentration of thiourea improves the films' growth texture because atoms of thiourea embedded in the structure of the film, making it more uniform.

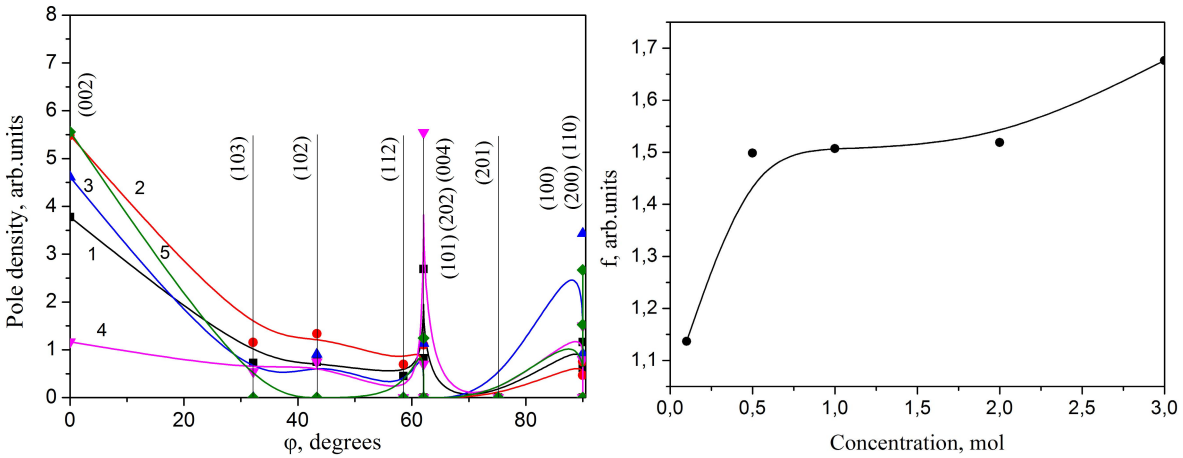

Figure 3. Pole density P_i, and orientation factor f, as a function of the incidence angle φ between the direction and the normal to the reflection plane for films obtained at different concentrations of thiourea (1 - 0.1 M, 2 - 0.5 M, 3 – 1 M, 4 – 2 M, 5 – 3 M)

Figure 4 shows the results of calculating the coherent scatter domain (CSD) in directions perpendicular to the crystallographic (100), (110) and (002) planes. These directions correspond to the crystal lattice axes of the hexagonal phase. We found that the CSD varies in the range of $L_{(100)}$ = (21-48) nm, $L_{(002)}$ = (38-60) nm, and $L_{(110)}$ = (21-36) nm. Furthermore, L has maximum value at the concentrations of thiourea of C = 0.1-0.5 mol. Increases of the thiourea concentration in the initial solution results in a monotonic decrease of the CSD size in all three directions. Others [14] obtained similar results in determining its size ($L_{(100),(002)}$ = 47-48 nm) using the Scherrer equation (grain shape factor K = 0.89).

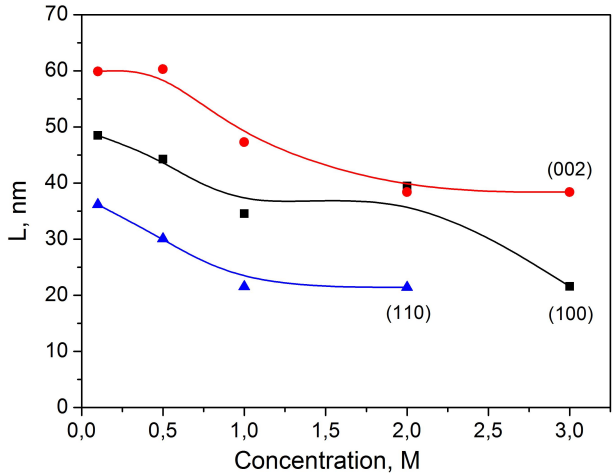

Figure 4. The effect of thiourea concentration on the CSD size in ZnO thin films. The CSD sizes in directions normal to the crystallographic (100), (110) and (002) planes were determined

Table 1 presents the results of calculating the lattice constants of ZnO condensates, made in solutions with different thiourea concentrations. Data were obtained by a graphical method of successive approximations after the first- and fifth-iteration. The value of the lattice constants *a, c* and the ratio *c/a* is practically unchanged after 4 and sometimes 5 iterations; this indicates convergence of the calculation for lattice parameters.

Table 1. Results of calculating ZnO lattice constants obtained by the iteration method using Nelson-Riley extrapolation graphs

C, M	1 iteration			5 iterations		
	a, nm	*c,* nm	*c/a*	*a,* nm	*c,* nm	*c/a*
0.1	0.32535	0.52119	1.601936	0.32525	0.52136	1.6029
0.5	0.32513	0.52094	1.602251	0.32488	0.52201	1.6067
1	0.32511	0.52262	1.607517	0.32401	0.52746	1.6279
2	0.32524	0.52138	1.603062	0.32503	0.52171	1.6051
3	0.32463	0.52143	1.606229	0.32466	0.52306	1.6111
Reference	a = 0.3256 nm; c = 0.5212 nm, c/a = 1.601 [15]					

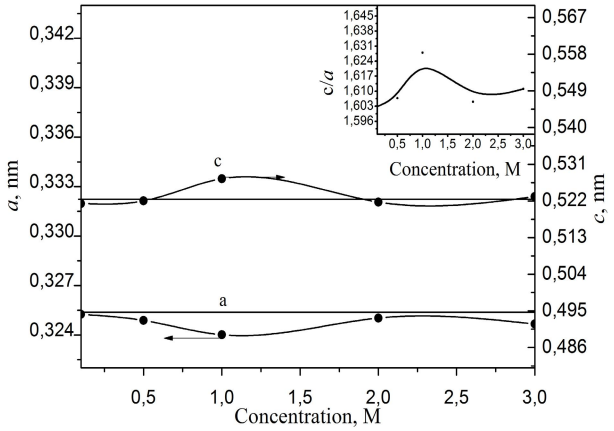

Figure 5. The effect of thiourea concentration on the lattice constants *a*, *c,* and *c/a.* The results of the fifth iteration for *c/a* are depicted in the inset

The dependence of *a, c,* and their ratio *c/a* as a function of thiourea concentration derived from the fifth iteration are shown in Figure 5. It was established that the lattice constants values for the material (a = 0.32466-0.32525 nm and c = 0.52171-0.52306 nm) are well correlated with data given in the reference [15] (a = 0.3256, c = 0.5212, and c/a= 1.601). Similar results of our calculation of lattice parameters (a = 0.325 nm and c = 0.521 nm) for zinc oxide films obtained by CBD from zinc acetate-dehydrate and sodium hydroxide solutions were found by others [15].

CONCLUSIONS

We obtained ZnO films by chemical-bath deposition in a solution of zinc sulfate, thiourea, and ammonia solution. Then, we assessed the dependence of the structural- and sub-structural- properties of the resulting condensates on the duration of the deposition and the concentration of thiourea in the initial solution. Furthermore, we showed that nanostructures form in the substrates during a 20-minute deposition. The optimal duration of deposition to assure the formation of a continuous layer is 60 min. Moreover, the films we generated display a hexagonal [002] growth texture, the quality of which depends on the concentration of thiourea. The average size of the CSD in directions corresponding to the axes of the crystal lattice of the hexagonal phase is equal to ($L_{(100)}$ = (21-48) nm, $L_{(002)}$ = (38-60) nm, $L_{(110)}$ = (21-36) nm); it decreases with increasing thiourea concentration in the initial solution. The films have lattice constants of a = 0.32466-0.32525 nm, c = 0.52171-0.52306 nm, and c/a=1.603-1.611. These values show a good correlation to reference films. In addition, we identified the best physical and technological conditions for obtaining continuous films with a single-phase structure and a relatively large CSD.

ACKNOWLEDGMENTS

This work is supported by the Ukraine State Agency for the Science, Innovation and Informatization and by the Ministry of Education and Science of Ukraine (Grant No. 0113U000131, 0112U000772). Two of us (Bolotnikov and James) were partially supported by the Department of Energy's NNSA Global Initiative of Proliferation Prevention and from the DOE/NNSA's Office of DNN R&D.

REFERENCES

[1] Wei, A., Pan, L., Huang, W., "Recent progress in the ZnO nanostructure-based sensors", Materials Science and Engineering B 176, 1409-1421 (2011).
[2] Özgür, U., Alivov, Ya. I., Liu, C., et al, "A comprehensive review of ZnO materials and devices", Journal of Applied Physics 89, 041301-1-103 (2005).
[3] Yevtushenko, A. I., Lashkaryov, G. V., Lazorenko, V. I., Karpina, V. A., Khranovskiy, V. D., "ZnO - UV detectors", Physics and Chemistry of Solids 9, 869-882 (2008) (In Ukrainian).
[4] Scheer, R., Werner Schock, H., [Chalcogenide Photovoltaics. Physics, Technologies, and Thin Film Devices], Wiley-VCH, Weinheim, 175-192 (2011).
[5] Rogozin, I. V., "Preparation of ZnO:N filmas by radical-beam gettering epitaxy method", Semiconductor Physics and Technology 41, 924-928 (2007) (In Russian).
[6] Tuomisto, F., Saarinen, K., Grasza, K., Mycielski, A., "Observation of Zn vacancies in ZnO grown by chemical vapor transport", Phys. stat. sol. 243, 794-798 (2006).
[7] Chitanu, E., Ionita, Gh., "Obtaining thin layers of ZnO with magnetron sputtering method", International Journal of Computers 4(4), 243-250 (2010).
[8] Bougrine, A., Hichou, A. E., Addou, M., Ebothé, J., Kachouane, A., Troyon, M., "Structural, optical and cathodoluminescence characteristics of undoped and tin-doped ZnO thin films prepared by spray pyrolysis", Materials Chemistry and Physics 80, 438–445 (2003).
[9] Kumari, V., Malik, B. P., Mohan, D., Mehra, R. M., "Laser Induced Nonlinear Optical Properties of Zinc Oxide Thin Film Prepared By Sol-Gel Method", J. Nano- Electron. Phys. 3, 601-609 (2011).
[10] Wang, H., Xie, C., "Controlled fabrication of nanostructured ZnO particles and porous thin films via a modified chemical bath deposition method", Journal of Crystal Growth 291, 187-195 (2006).
[11] Ortega-Lopez, M., Avila-Garcıa, A., Albor-Aguilera, M. L., Sanchez Resendiz, V. M., "Improved efficiency of the chemical bath deposition method during growth of ZnO thin films", Materials Research Bulletin 38, 1241-1248 (2003).
[12] Shinde, V. R., Lokhande, C. D., Mane, R. S., Han, S.-H., "Hydrophobic and textured ZnO films deposited by chemical bath deposition: annealing effect", Applied Surface Science 245, 407-413 (2005).
[13] Wang, M., Hahn, S. H., Kim, J. S., Hong, S. H., Koo, K.-K., Kim, E. J., "Chemical bath deposition of textured ZnO thin films in aqueous/ethanolic solution", Materials Letters 62, 4532-4534 (2008).
[14] Yi, S.-H., Choi, S.-K., Jang, J.-M., Kim, J.-A., Jung, W.-G. "Low-temperature growth of ZnO nanorods by chemical bath deposition", Journal of Colloid and Interface Science 313, 705-710 (2007).
[15] Wu, Z. Y., Cai, J. H., Ni, G., "ZnO films fabricated by chemical bath deposition from zinc nitrate and ammonium citrate tribasic solution", Thin Solid Films 516, 7318-7322 (2008).
[16] Warren, B. E., [X-ray Diffraction. Dover], New York, 253 p. (1990).
[17] [Selected powder diffraction data for education straining (Search manual and data cards)], Published by the International Centre for diffraction data, USA, p. 432 (1997).
[18] Umanskij, Ja. S., Skakov, Ju. A., Ivanov, A. N., Rastorgujev, L. N., [Crystallogaphy, X-ray graph and electronmicroscopy], Metallurgy, Moskow, 632 p. (1982) (in Russian).
[19] Opanasyuk, A. S., Kurbatov, D. I., Kosyak, V. V., Kshniakina, S. I., Danilchenko, S. N., "Characteristics of structure formation in zinc and cadmium chalcogenide films deposited on nonorienting substrates", Crystallography Reports 57, 927-933 (2012).
[20] Berestok, T. O., Kurbatov, D. I., Opanasyuk, N. M. , Pogrebnjak, A. D., Manzhos, O. P., Danilchenko, S. M., "Structural properties of ZnO thin films obtained by chemical bath deposition technique", Journal of Nano- and Electron Physics 5(1), 01001-01004 (2013).
[21] Kosyak, V. V., Kurbatov, D. I., Kolesnyk, M. M., Opanasyuk, A. S., Danilchenko, S. N., Gnatenko, Yu. P. "Structural and electrical properties of ZnS/CdTe and ZnTe/CdTe heterostructures", Journal of Materials Chemistry and Physics 138, 731-736 (2013).